Do Intermediate Gaits Matter When Rapidly Accelerating?

Callen Fisher, *Student Member, IEEE*, Christian Hubicki, *Member, IEEE*, and Amir Patel, *Member, IEEE*

***Abstract*—Transient locomotion is still poorly understood in terms of planning and implementation on robotic platforms, with most research concentrated on steady-state motion. In this letter, we investigate optimal rapid acceleration (positive and negative) maneuvers of a planar numerical quadruped and biped robot. The question we ask is whether legged robots should transition through discrete, intermediate gaits (walking to trot to bound) or plan a direct transition to the top-speed gait. We present numerical evidence supporting the energetic optimality of transitioning to a desired gait without intermediate gait transitions. Trajectories were generated from rest to steady state and vice versa. Two cost functions (cost of transport and a heat-based cost function) were analyzed and compared to observations made in nature. A full 30-m trajectory was generated and compared to the acceleration and deceleration results, which further supported transitioning directly to the desired gait. All the trajectories were observed to follow a sliding mass template model which, in future, can be used as a heuristic to plan these transient maneuvers.**

***Index Terms*—Legged robots, optimization and optimal control, under actuated robots.**

I. Introduction

LEGGED robots will need to be agile in order to operate robustly outside the lab. However, rapid acceleration (and transient locomotion in general) has not been thoroughly studied in robotics. It has been shown that trajectories generated using trajectory optimization methods require less energy than the SLIP (spring loaded inverted pendulum) based Raibert controllers [1] which are prevalent in the literature. The trajectory optimization literature has largely been focused on analyzing different gaits (footfall patterns [2], [3]) and their energy efficiency (in terms of cost of transport, CoT) at different velocities in legged robots [2], [4], [5].

The current robotic literature often uses simplified models that reveal the centre of mass (COM) motion for steady state gaits (such as the SLIP model [6], [7]). However these templates designed for steady-state motions will not hold when they are applied to rapid acceleration maneuvers. These models often have massless legs [3], [6], point mass bodies [3], [8], infinite friction with no foot slipping [5], [6] and sometimes have infinite power for their actuators [9]. Further, these optimizations are often seeded with gait patterns [5], [7] or have the foot contact order enforced [2], [3], [5], [6]. Therefore the motions that are generated do not naturally emerge from the optimizer. Presently, there is an ongoing debate on when and how a robot should change its gait pattern [10] (gait transition[1]). Some robotic studies [2], [4] have achieved acceleration by slowly increasing the forward velocity until a certain Froude number is reached, that is in the region of attraction of the new gait, and then switch to the new gait controller. These transitions are often done by optimizing different portions of the trajectory and stitching the results together [11] (effectively forcing a gait transition as a combination of discrete, intermediate gaits[2]). In some cases acceleration is achieved by stitching two gaits together using polynomials [11]. However a complete trajectory from rest to top speed has not been optimized to see if these gait transitions (with slowly increasing forward velocity) naturally emerge. A similar study has been performed where human subjects were told to slowly increase their walking speed until it was more comfortable to run [12]. The aim was to determine the speed where gait transitions occur, however energy efficiency was not measured.

One can turn to nature for a possible answers to the question: **Should multiple gait transitions be used when rapidly accelerating?** From observing video footage along with the relevant literature on the cheetah (*Acinonyx jubatus*) [13] and greyhound (*Canis familiaris*) [14], [15] during transient locomotion, it is evident that from rest they accelerate straight into a gallop and do not use any intermediate gaits such as walk and trot to get there. In humans, Long and Srinivasan[16] performed experiments where subjects were given a stop watch and were told to cover a fixed distance to arrive in a fixed time. It was noted for long time periods the subjects walked the entire distance, for shorter time periods the subject performed a combination of walking and running (multiple gait changes, with one transition from rest to walk and walk to run being optimal) and for short time periods the subject ran the entire distance, accelerating straight into the run gait.

Manuscript received February 24, 2019; accepted June 14, 2019. Date of publication July 9, 2019; date of current version July 19, 2019. This letter was recommended for publication by Associate Editor J. Yi and Editor D. Song upon evaluation of the reviewers' comments. This work was supported by the National Research Foundation of South Africa under Grants 99380 and 101245. *(Corresponding author: Callen Fisher.)*

C. Fisher and A. Patel are with the Faculty of Electrical Engineering, University of Cape Town, Cape Town 7700, South Africa (e-mail: fshcal001@myuct.ac.za; a.patel@uct.ac.za).

C. Hubicki is with the Faculty of Mechanical Engineering, Florida State University, Tallahassee, FL 32310-5754 USA (e-mail: hubicki@eng.famu.fsu.edu).

Digital Object Identifier 10.1109/LRA.2019.2927952

[1]Gait transition: transitioning from one periodic discrete footfall pattern to another. For example: transitioning from a bound to a gallop independent of the velocity.

[2]For example optimize the discrete intermediate walking and running gaits, and then stitch them together (rest to walk and then walk to run) to form the complete acceleration trajectory.

This raises some questions:

- Is it energetically optimal to rather accelerate straight to the highest speed gait instead of performing multiple intermediate gait transitions?
- Is there a template or heuristic that can be used to plan these non-steady energy optimal acceleration trajectories?

The focus of this letter is to provide insight into these questions by generating energetically optimal trajectories for rapid acceleration that naturally emerges without prescribing contact order. Here we show that multiple intermediate gait transitions are not energetically optimal and only the highest velocity gait is required for a legged robot to accelerate. Additionally, we demonstrate that across both bipeds and quadrupeds a reduced order (template) model for transient locomotion emerges. We believe that this model could potentially be used for long-time-horizon motion planning.

This letter begins by describing the models and experimental method in Section II which includes the details of the trajectory optimization techniques employed. The results and discussion are then presented in Section III and IV. A detailed explanation of the emerging template and how it can be used is presented in Section IV-A. The letter ends with the conclusions and future work described in Section V.

II. Method

In order to analyze these transient motions, trajectories were generated and analyzed to determine the optimal method for rapid acceleration and deceleration. Energy efficiency is an important objective in robotics [17] and two different energy based cost functions were analyzed and compared. As rapid transients often occur in time-constrained environments, the maximum time to perform these maneuvers was varied to gain insight into how time effects these maneuvers.

Two different models were optimized and the results were compared for similarities and trends emerging between legged morphologies. The models are planar (constrained to the sagittal plane) and include a biped and a quadruped as seen in Fig. 1. The literature supports bounding in planar quadruped robots[3] [18]. The equations of motion were calculated using Euler-Lagrange dynamics (in the form of the manipulator equation) as follows:

$$\mathbf{M}(\mathbf{q})\ddot{\mathbf{q}} + \mathbf{C}(\mathbf{q},\dot{\mathbf{q}})\dot{\mathbf{q}} + \mathbf{G}(\mathbf{q}) = \mathbf{B}\boldsymbol{\tau} + \mathbf{A}\boldsymbol{\lambda} \qquad (1)$$

where $\mathbf{q}$ are the generalized coordinates (with absolute angles for each rigid body). $\boldsymbol{\lambda}$ is the ground reaction forces and $\boldsymbol{\tau}$ are the generalized torques from the actuators.

Steady-state trajectories (a run for the biped and bound for the quadruped, at an average centre of mass velocity of 5 m/s) were first generated for the biped and quadruped robot. Then acceleration trajectories were generated from rest to the apex of the respective steady-state trajectory (where $\dot{z} = 0$) in a constrained maximum time and vice versa for the deceleration

[3]It is hypothesized that this is partly due to the fact that it is a planar model and it is suspected that galloping requires an actuated spine [6] and we further hypothesize that a model that can roll its spine in the frontal plane might also be required.

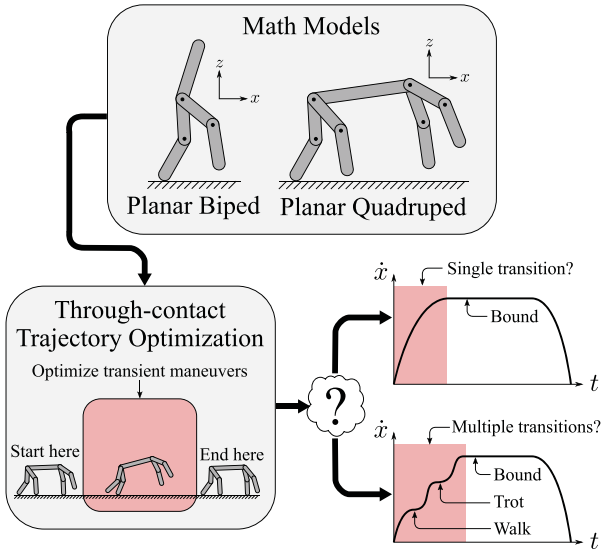

Fig. 1. The two models (quadruped and biped) that were investigated for this research are shown above. The motion of interest was the rapid acceleration and deceleration phases. The aim of the study was to investigate these transient motions and to gain insight into how these motions are performed in robotic platforms. The main focus is to determine if it is energetically optimal to jump straight into the highest speed gait or to perform multiple intermediate gait transitions.

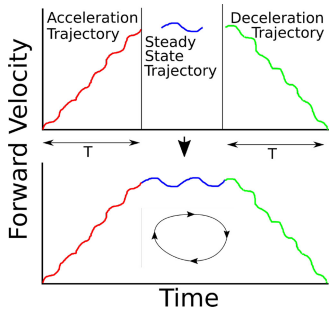

Fig. 2. As the transient motions (rapid acceleration and deceleration) were of interest, it was decided to break the trajectory (long-time-horizon trajectory) into three phases. These phases included the acceleration, steady-state (limit cycles so that multiple trajectories could be *stitched* together) and the deceleration phase, as seen in the above figure. This allowed for smaller and more accurate (more finite elements) problems to be solved and then the results were *stitched* to form the long-time-horizon trajectory.

trajectories. A number of experiments were run for different maximum time periods (T).

These acceleration and deceleration trajectories were then stitched to the steady-state trajectories. These stitched trajectories made a complete run starting and ending at rest with an acceleration, steady-state and deceleration phase in the motion as seen in Fig. 2. This ensured that the robots accelerated and decelerated to and from a feasible gait. Two different cost functions were optimized, the cost of transport (CoT) cost function (J1)[4] and a heat based torque squared cost function (J2).

$$J_1 = \int_{t=0}^{T_{total}} \frac{\tau(t)^2}{x_{\text{final}}} dt \quad J_2 = \int_{t=0}^{T_{total}} \tau(t)^2 dt \qquad (2)$$

[4]J1 is not a true CoT and is a heat based cost normalized by the distance travelled. However it is proportional to the non-dimensional cost of transport.

where T_{total} is the maximum transition time and x_{final} is the final distance covered. For the steady-state trajectories, 10 trajectories were generated and the optimal (in terms of CoT) was chosen. Then 5 acceleration and deceleration trajectories for each cost function were generated for a number of different time periods ($T \in [2, 3, 4, 5, 6]$ seconds). The optimal CoT and heat cost trajectories, for each time period, were chosen and analyzed. By having a single steady-state step (only the CoT cost function was used to generate the steady-state step), the transient trajectories had the same start and end points allowing the effect of the different cost functions to be isolated.

These trajectories were generated using trajectory optimization methods. Trajectory optimization is a mathematical tool used to solve complex nonlinear problems that are required to satisfy a number of constraints and bounds, while minimizing a specified cost function. This is achieved by varying the decision variables between their respective bounds, until an optimal solution is found. All trajectory optimization problems follow a general framework that is well described in the tutorial by Kelly [19]. The constraints and bounds, along with the problem set-up is detailed below.

A. Constraints

To help the solver find a kinematically feasible trajectory, there are a number of constraints that are enforced. These guide the solver to a solution and are described below:

1) Direct-Collocation: Each state trajectory was discretized into N time periods (finite elements) using polynomials. N varied according to what was being optimized (50 for the steady-state steps and 150 for the acceleration and deceleration trajectories). The trajectories are represented using a Runge-Kutta basis with K- collocation points [20]. In this case 3 point Radau (with an accuracy of h^{2K-1}) was used to solve the differential equations, (1), at the selected points in time [20], [21].

The time between the end points (mesh points) of the elements was governed by the following constraint:

$$0.5h_M \leq h_i \leq 2h_M \tag{3}$$

where h_i is the time period for the i^{th} finite element and h_M is set to $T/(N)$. T was varied according to the time bounds of the task that was being optimized (see Section II-A6).

2) Contact-Implicit Optimization Method: To avoid limiting non-intuitive solutions, a gait pattern was not enforced (for the acceleration and deceleration trajectories, however it was enforced when generating the steady-state trajectories). Contact-implicit optimization methods [22] allow the optimizer to determine the best foot contact order for a given trajectory. These methods have shown to be a vital tool in studying locomotion [23], [24]. Recently, orthogonal collocation has been applied to contact-implicit optimization, which has significantly increased its accuracy [20]. This method does require a large number of complementarity constraints that can be found in [22] equation (8) to (16). All contacts were modelled as an inelastic collision [1], [22] and slipping was modelled using a coulomb friction model [22]. In order to solve these inherently difficult complementarity constraints, the ϵ-relaxation method [25] was used as follows:

$$\begin{gathered} \alpha_i' \beta_i' < \epsilon \\ \alpha_i' = \sum_{j=0}^{K} \alpha_{ij} \qquad \beta_i' = \sum_{j=0}^{K} \beta_{ij} \end{gathered} \tag{4}$$

where α_{ij} and β_{ij} form the two parts of the complementary constraints for the i^{th} node and j^{th} collocation point and ϵ is a relaxation parameter. These variables are summed across the collocation points and evaluated at the mesh point (instead of ever collocation point, drastically simplifying the problem).

3) Joint Angles: Due to the use of absolute angles, constraints on the relative joint angle were used to limit the motion of the limb to a feasible range as follows:

$$\begin{gathered} \text{lower bound} < \theta_{\text{hip}} - \theta_{\text{spine}} < \text{upper bound} \\ \text{lower bound} < \theta_{\text{knee}} - \theta_{\text{hip}} < \text{upper bound} \end{gathered} \tag{5}$$

The knees were allowed a relative rotation of 100° and the hips were allowed a relative rotation of 180°. Similar constraints were applied to the relative velocity of the limbs.

4) Motor Model: In order to limit the power of the robots, a simple motor model (representing a linear torque-angular velocity relationship) was implemented which limited the available torque according to the relative velocity of the limb as follows [26]:

$$-\tau_{\text{max}} - \frac{\tau_{\text{max}}}{\omega_{\text{max}}}\omega \leq \tau \leq \tau_{\text{max}} - \frac{\tau_{\text{max}}}{\omega_{\text{max}}}\omega \tag{6}$$

5) Initial and Terminal Conditions: The initial and terminal conditions varied according to the problem being optimized as follows:

- Steady-state trajectories: The initial conditions were left unconstrained (except for the vertical velocity, $\dot{Z}$, being forced to zero for the apex point). The terminal conditions were set to equal the starting values through constraints (except for the horizontal position, X) to ensure periodicity.
- Acceleration trajectories: The initial conditions were set by constraining the first point to be the rest configuration of the robot with zero velocities. The terminal conditions were enforced through constraints to match the apex of the optimal steady state trajectory (X was left free).
- Deceleration trajectories: The initial conditions were set by constraining the first point to the apex of the steady-state trajectory. The terminal conditions were enforced through constraints to match the rest configuration of the robot with zero velocity (X was left free).

6) Maximum Transition Time Constraints: For the acceleration and deceleration trajectories, an upper bound on the maximum transition time was enforced. This meant that it had to complete the acceleration/deceleration phase within a prescribed time. This was enforced using the following constraint:

$$\sum_{i=0}^{N} h(i) < T \tag{7}$$

where $T \in [2, 3, 4, 5, 6]$ seconds.

B. Bounds

Bounds are applied to all decision variables in order to restrict the search space. These bounds were chosen carefully in order to not eliminate any non-intuitive solutions. The decision variables available to the optimizer are as follows:

$$decVar = \left[\mathbf{q}, \dot{\mathbf{q}}, \ddot{\mathbf{q}}, \boldsymbol{\tau}, \mathbf{h}, \boldsymbol{\lambda}, \mathbf{slack}\right] \tag{8}$$

where $\mathbf{q}$ (and its derivatives), $\boldsymbol{\lambda}$ and $\boldsymbol{\tau}$ form part of the equations of motion, (1). In order to solve the complementarity constraints, a number of slack variables are needed [22]. Variables that are not bounded through constraints are bounded sufficiently high so as to not eliminate any viable solutions.

C. Solver Set-Up and Seed Generation

Due to the complexity and non-linearity of the problem that needs to be solved, there is no guarantee that the solver will find an optimal solution the first time it is run and may get stuck in the many local minima. Therefore to increase the likelihood that the solver will find the true optimal result, a number of optimization problems were run from a randomly generated starting point (called a seed point) and the best solution was used as the optimal solution. These seed points are generated using uniformly distributed random numbers between the bounds of the decision variables.

However, a number of heuristics were employed to improve the convergence rate and time [20], [27]. One such method was to only randomize the generalized coordinates of the robot and to set rest of the decision variables to 0.01 [28].

Another was to solve the seed point iteratively, each time adding more constraints, with the cost function set to a fixed value and the required tolerances being set fairly low [20]. Once all constraints had been added, the solver was warm started with tighter tolerances and the actual cost function, (2), being minimized.

Due to the complementarity constraints from the contact-implicit method, the ϵ-relaxation technique was employed [25]. Initially, ϵ was set to 1000 and the problem was solved iteratively, 8 times, with each iteration ϵ was divided by 10. As soon as an optimal solution could not be found for one of the iterations, the seed was abandoned and the next seed point was run. After 8 successful solve iterations, the complementarity constraints, (4), were considered satisfied ($\epsilon = 1E-4$) and the solution was saved [25]. GAMS (General Algebraic Modelling System) [29] software along with the IPOPT [30] solver was used for the optimization.

III. Results

The results are divided into two sections. These are detailed below and include the acceleration and deceleration trajectories. Animations of the results can be found here: https://youtu.be/QhJD2Es7UlU

A. Acceleration Trajectories

The optimal acceleration trajectories for the biped and quadruped for each time period were analyzed and the COM velocity plots for the shortest (maximum transition time of 2 seconds) and longest time (maximum transition time of 6 seconds), for both cost functions can be seen in Fig. 3.

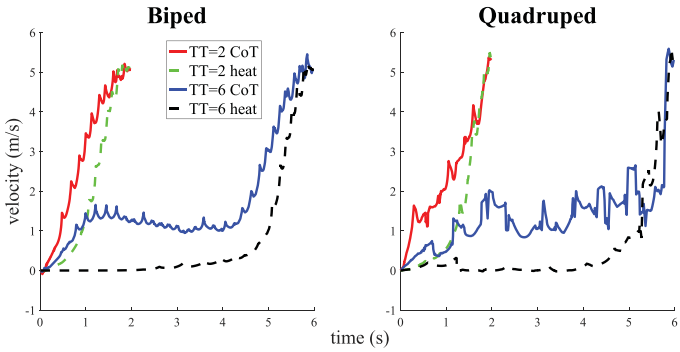

Fig. 3. The acceleration COM velocity plots for both models and both cost functions are presented for two time periods: 2 seconds and 6 seconds. For the longer time periods the CoT results are seen to perform a gait transition and a walking gait emerges before accelerating to the highest speed gait. For the heat based cost function, the robots were observed to stay at rest until the last moment and then leap straight into the highest speed gait.

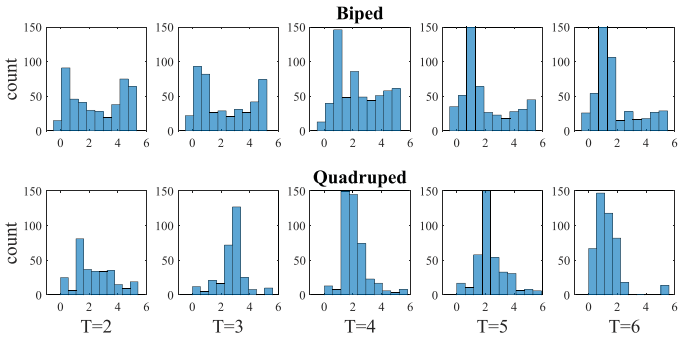

Fig. 4. Bar graph of the COM velocity of the different acceleration time periods (for both models and CoT cost function) reveals how as the time period increases, more time is spent at lower speeds for the CoT trajectories. This matches results in [16]. The Y axis represents the number of node points corresponding to the velocity range (X axis).

A walking gait naturally emerges (one foot always on the ground) for the CoT trajectories for the longer time period (6 seconds). A bar graph showing the velocities for the acceleration maneuvers for different time periods for the CoT trajectories are shown in Fig. 4. This shows that as the time increases more time is spent at lower speeds. For the CoT acceleration trajectories with a maximum transition time of 6 seconds, the robots remained grounded (walking) until the biped reached 2.3 m/s and the quadruped reached 1.7 m/s. This resulted in the biped walking for 80% of the time and 81% of the time for the quadruped.

B. Deceleration Trajectories

The optimal deceleration trajectories for the shortest (maximum transition time of 2 seconds) and longest time period (maximum transition time of 6 seconds), for both cost functions can be seen in Fig. 5. Once again the walking gait emerges for the CoT trajectory with a long time period. For these trajectories the

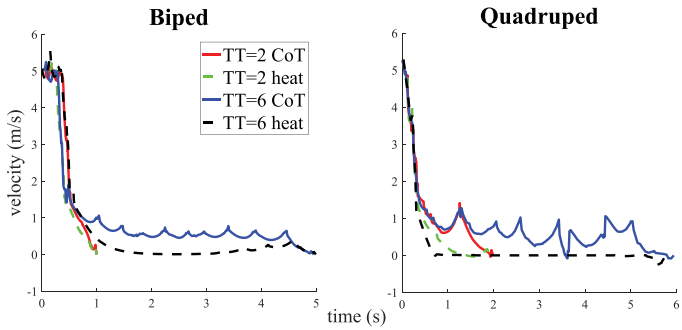

Fig. 5. The deceleration trajectories COM velocity plots for both models and both cost functions for the time period of 2 seconds and 6 seconds are shown in the above graph. For the CoT a walking gait emerges before decelerating to rest. For the heat based cost function the robot decelerates to rest and remains stationary for the remainder of the time.

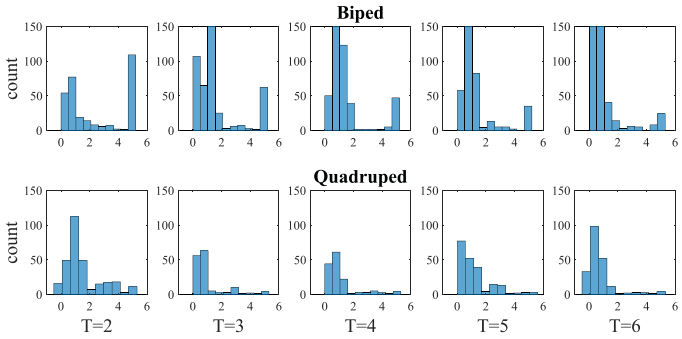

Fig. 6. Bar graph of the COM velocity of the different time periods (for both models and CoT cost function) shows how as the time period increases, more time is spent at lower speeds. Once again matching results in [16]. The Y axis represents the number of node points corresponding to the velocity range (X axis).

biped began walking at 1.7 m/s and quadruped from 1.37 m/s. This resulted in the biped walking for 92% of the time and 93% of the time for the quadruped.

A bar graph showing the velocities for the deceleration trajectories for different time periods for the CoT cost function are shown in Fig. 6. The bar graph reveals that as the time increases, more time is spent at lower speeds.

IV. Discussion

A number of acceleration and deceleration trajectories were generated and stitched to the optimal steady-state trajectory for both the biped and quadruped robot. Two cost functions were optimized over different time periods. The acceleration and deceleration trajectories required multiple steps. The biped requires 10 steps to accelerate and 3 steps to decelerate. The quadruped requires 8 steps to accelerate and 3 steps to decelerate. However these were considered as a single transition as no periodic limit cycle behaviour was observed during the transition. These transitions from rest to the highest speed took approximately two seconds (compared to approximated 0.3 seconds for the complete steady-state step).

The results revealed some interesting trends across the two models. In both models, for short time periods the robots launched straight into the desired high speed gait (or straight to rest for the deceleration trajectories) and did not perform intermediate gaits as is often done in the robotics literature [4], [32]. Similar results were revealed when studying animals, such as the cheetah [13] and greyhound [14], [15], where the animals jump straight into their highest speed gait when rapidly accelerating.

As the time period increased, a walking gait emerges in the CoT trajectories, until the last moment where the robots launched straight into the desired gait. We call this walking gait the slowest walk, as it is the slowest optimal gait that emerges. The same motion occurred for the deceleration trajectories, where the robot immediately decelerated to the slowest walk and then at the last moment it stopped in a rest configuration.

Studying the slowest walk, which naturally emerges as the energy optimal solution for long time periods, it was observed that the walk remains at a roughly constant velocity and does not slowly increase before transitioning to the new gait pattern. Studies on humans walking on treadmills have shown that increasing your walking velocity significantly increases metabolic costs [8], which reveals that remaining at a constant speed, like the slowest walk, is optimal. Often in the robotics literature the velocity will be increased to a set Froude number where it will be in the attraction region of the new gait's limit cycle [2], [33], then transition to a different gait's controller, which, as shown in these results, is not optimal.

Multiple combinations of intermediate gaits could have been enforced using constraints and compared to the above results to determine the optimal trajectory. However this was circumvented by using contact-implicit optimization methods.

Intuitively, for the heat cost functions the robots would stand stationary and at the last minute leap to the desired gait. Similarly, for the deceleration task, it would decelerate to rest as soon as possible and then stand stationary for the duration of the time period, which naturally emerged.

For all the results, the robots would leap (either from rest or from the slowest walk) to the desired gait and would not perform multiple intermediate gait transitions. There is a concern about the required power output to achieve these trajectories as this power must be provided by the power source and actuators of the robot. The mechanical structure must also be capable of transferring this power from the actuators to a forward velocity. Previous studies have shown that transient motion requires special design considerations [23], [31].

In order to determine what naturally emerges from the optimization without stitching multiple trajectories together (enforcing steady-state locomotion), a full trajectory (long-time-horizon trajectory, with $N = 300$) was optimized where the robot had to start and end at rest and travel a fixed distance (30 m.) in a fixed time period. The COM velocity plots can be seen in Fig. 7. These results validate what is observed in the acceleration and deceleration trajectories, where the robots are seen to accelerate straight into the highest velocity gait and decelerate straight to rest.

To validate the need for these complex optimization methods (contact-implicit optimizations with allowed foot slipping) the effective coefficient of friction, λ_x/λ_z, was calculated (for a biped acceleration trajectory) and is shown in Fig. 8. It was

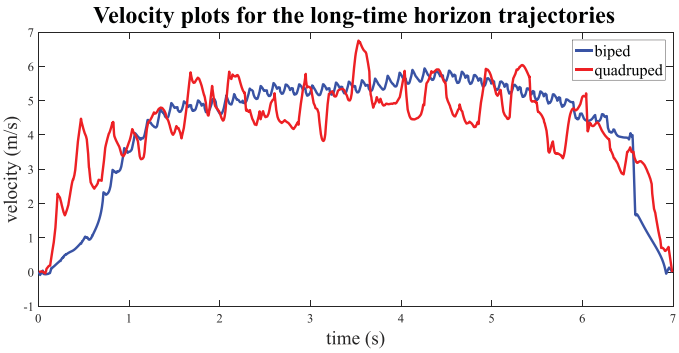

Fig. 7. Note how the acceleration and deceleration phases of the above COM velocity plots for the biped and quadruped long-time-horizon trajectories closely relate to the results in Fig. 3 and 5, with the robot accelerating straight to the highest velocity gait. These trajectories took much longer to converge (over 4 hours) compared to the quick stitching results (each phase took about 15 minutes). Due to the size of this problem, only 300 node points were used whereas for the stitched results, 150 nodes were used for each transient phase and 50 nodes for each steady-state step, improving the resolution and accuracy of the stitched results.

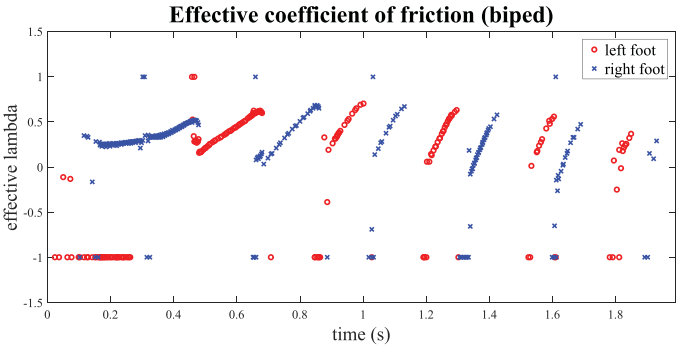

Fig. 8. The effective friction during an acceleration trajectory for the biped robot reveals that it often clips at one, indicating that the foot starts to slide. This shows that infinite friction and enforcing a no-slipping condition are not valid assumptions and these contact-implicit optimization methods need to be implemented.

observed to often clip the maximum surface coefficient of friction (set to 1 in these optimizations). At this point, the foot was slipping.

A. *Significance to Robotics*

From analyzing the COM velocity plots for the long-time-horizon results (Fig. 7) and the stitching results (Fig. 3 and 5), one can see indications of "bang-coast-bang" like control emerging in these maneuvers [34]. Bang-coast-bang is most iconically attributed to a minimum time control of a sliding mass with an external horizontal force being applied in the presence of viscous friction [28].

In [28] it was shown that a sliding mass profile emerged when optimizing a simple monopod model for long-time-horizon trajectories and it was hypothesized that this template may hold for other, more complex models. The velocity plots from the above results all reveal the sliding mass template. The profile is followed during the gait transitions (from rest to top speed, from rest to walk and from walk to top speed) for the acceleration and deceleration phases and thus holds for both complex models.

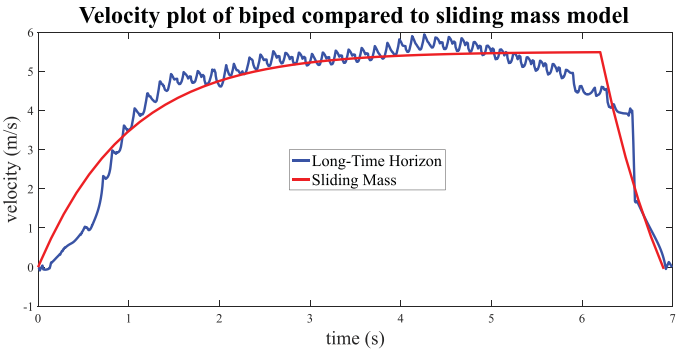

Fig. 9. The sliding mass profile compared to the long-time-horizon velocity plot shows that this single degree of freedom model accurately predicts the velocity profile for these rapid transient maneuvers. The template can be used as a heuristic to plan these maneuvers and will enable online real time planning.

The sliding mass model obeys the following dynamics:

$$\ddot{x} = \frac{F(t) - c\dot{x}}{m} \tag{9}$$

where $F(t)$ is the time varying applied force, c is the viscous friction, m is the mass of the sliding mass and $\dot{x}$ is the horizontal velocity of the mass. The velocity profile is shown in Fig. 9 and is compared to the long-time-horizon velocity plot. The applied force was hand-tuned until the sliding mass model fitted the velocity profile of the long-time-horizon trajectory.

In terms of robotics, these results are significant when generating trajectories and controllers for rapid acceleration or deceleration maneuvers. The use of the simple template as a heuristic will allow for much faster long-time-horizon trajectory planning capable of running in real time with lower level PD controllers used to control the limbs to track the velocity set-point generated by the sliding mass template.

B. *Significance to Biology*

It is encouraging that these results match observations made in nature, which therefore indicates that animals are inherently minimizing a CoT cost function when performing these rapid maneuvers. Animals are seen to jump straight into the highest speed gait and avoid multiple gait transitions due to the cost of transitioning [16], which matches observations made in these results.

Similar biological observations were made in [16] where human subjects had to cover a fixed distance in a fixed time. It was noted that when the time was short the subjects ran the whole distance, accelerating straight to the running gait, matching results achieved in this letter. [16] also noted that when a cost was included for gait transitions, it was optimal to make only one transition.

V. Conclusion and Future Work

In this letter we have demonstrated that it is energetically optimal to accelerate from rest straight into the desired gait and to avoid multiple intermediate gait transitions. Results showed that it is energetically optimal to move at the optimal speed of the

gait and to avoid slowly increasing the speed to a certain Froude number to initiate a transition. The sliding mass template model was observed to always emerge and can therefore be used as a heuristic to plan these maneuvers.

It is encouraging that these results emerged from trajectory optimizations that made use of complex realistic models that did not fix the foot contact order and allowed for foot slipping. Further, these trajectories emerged naturally from random seed points and were not seeded with a gait pattern.

Energy optimal gaits (CoT and heat based cost) were a focal point of this research as minimizing transportation costs is a fundamental goal towards achieving autonomy in robotics [17]. There is copious evidence from studies based on models [35] that minimizing energy costs is a high priority for locomotion in legged robots. Two questions were proposed in this letter and are answered as follows:

- Is it energetically optimal to rather accelerate straight to the highest speed gait instead of performing multiple intermediate gait transitions? Our results support the hypothesis that it is indeed energetically optimal to accelerate straight to the highest speed gait and these results emerged from contact-implicit optimizations.
- Is there a template or heuristic that can be used to plan these non-steady energy optimal acceleration trajectories? The sliding mass template naturally emerges for all the gait transitions for both models and can be used as a heuristic for real-time planners.

Future work will include exploring whether these results will extend from planar models to 3D.

REFERENCES

[1] J. Yu, D. Hong, and M. Haberland, "Energetic efficiency of a compositional controller on a monoped with an articulated leg and SLIP dynamics," in *Proc. IEEE/RSJ Int. Conf. Intell. Robots Syst.*, 2018, pp. 2221–2228.

[2] D. Hyun, J. Lee, S. Park, and S. Kim, "Implementation of trot-to-gallop transition and subsequent gallop on the MIT Cheetah 1," *Int. J. Robot. Res.*, vol. 35, no. 13, pp. 1627–1650, 2016.

[3] Z. Gan, Z. Jiao, and C. Remy, "On the dynamic similarity between bipeds and quadrupeds: A case study on bounding," *IEEE Robot. Autom. Lett.*, vol. 3, no. 4, pp. 3614–3621, Oct. 2018.

[4] D. Owaki and A. Ishiguro, "A quadruped robot exhibiting spontaneous gait transitions from walking to trotting to galloping," *Sci. Rep.*, vol. 7, no. 1, 2017, Art. no. 277.

[5] W. Xi, Y. Yesilevskiy, and C. Remy, "Selecting gaits for economical locomotion of legged robots," *Int. J. Robot. Res.*, vol. 35, no. 9, pp. 1140–1154, 2016.

[6] T. Kamimura, S. Aoi, K. Tsuchiya, and F. Matsuno, "Body flexibility effects on foot loading in quadruped bounding based on a simple analytical model," *IEEE Robot. Autom. Lett.*, vol. 3, no. 4, pp. 2830–2837, Oct. 2018.

[7] H. Celik and S. Piazza, "Simulation of aperiodic bipedal sprinting," *J. Biomech. Eng.*, vol. 135, no. 8, 2013, Art. no. 081008.

[8] N. Seethapathi and M. Srinivasan, "The metabolic cost of changing walking speeds is significant, implies lower optimal speeds for shorter distances, and increases daily energy estimates," *Biol. Lett.*, vol. 11, no. 9, 2015, Art. no. 20150486.

[9] J. Usherwood, "Inverted pendular running: A novel gait predicted by computer optimization is found between walk and run in birds," *Biol. Lett.*, vol. 6, pp. 765–768, 2010.

[10] T. Hubel and J. Usherwood, "Vaulting mechanics successfully predict decrease in walk-run transition speed with incline," *Biol. Lett.*, vol. 9, no. 2, 2013, Art. no. 20121121.

[11] O. Kwon and J. Park, "Gait transitions for walking and running of biped robots," in *Proc. IEEE Int. Conf. Robot. Autom.*, 2003, pp. 1350–1355.

[12] I. van Caekenberghe, K. De Smet, V. Segers, and D. De Clercq, "Overground vs. treadmill walk-to-run transition," *Gait Posture*, vol. 31, pp. 420–428, 2010.

[13] Cheeetah Running. [Online]. Available: https://youtu.be/mufJyH7qRpI. Accessed on: Feb. 21, 2019.

[14] R. Gillette and T. Angle, "Recent developments in canine locomotor analysis: A review," *Veterinary J.*, vol. 178, pp. 165–176, 2008.

[15] R. Walter and D. Carrier, "Rapid acceleration in dogs: Ground forces and body posture dynamics," *J. Exp. Biol.*, vol. 212, pp. 1930–1939, 2009.

[16] L. Long and M. Srinivasan, "Walking, running, and resting under time, distance, and average speed constraints: Optimality of walk-run-rest mixtures," *J. Roy. Soc. Interface*, vol. 10, no. 81, 2013, Art. no. 20120980.

[17] S. H. Collins, A. Ruina, R. Tedrake, and M. Wisse, "Efficient bipedal robots based on passive-dynamic walkers," *Science*, vol. 307, no. 5712, pp. 1082–1085, 2005.

[18] R. Alexander, "Why mammals gallop," *Amer. Zoologist*, vol. 28, no. 1, pp. 237–245, 1988.

[19] M. Kelly, "Transcription methods for trajectory optimization: A beginners tutorial," Cornell University, Ithaca, NY, USA, 2015.

[20] A. Patel, S. Shield, S. Kazi, A. Johnson, and L. Biegler, "Contact-implicit trajectory optimization using orthogonal collocation," *IEEE Robot. Autom. Lett.*, vol. 4, no. 2, pp. 2242–2249, Apr. 2019.

[21] L. Biegler, *Nonlinear Programming: Concepts, Algorithms, and Applications to Chemical Processes*, vol. 10. Philadelphia, PA, USA: SIAM, 2010.

[22] M. Posa, C. Cantu, and R. Tedrake, "A direct method for trajectory optimization of rigid bodies through contact," *Int. J. Robot. Res.*, vol. 33, no. 1, pp. 69–81, 2014.

[23] A. Blom and A. Patel, "Investigation of a bipedal platform for rapid acceleration and braking manoeuvres," in *Proc. IEEE Int. Conf. Robot. Autom.*, 2018, pp. 426–432.

[24] N. Doshi, K. Jayaram, B. Goldberg, Z. Manchester, R. Wood, and S. Kuindersma, "Contact-implicit optimization of locomotion trajectories for a quadrupedal microrobot," in *Proc. Robot., Sci. Syst.*, 2018.

[25] D. Ralph and S. Wright, "Some properties of regularization and penalization schemes for MPECs," *Optim. Methods Softw.*, vol. 19, no. 5, pp. 527–556, 2004.

[26] M. Haberland and S. Kim, "On extracting design principles from biology: II. Case study-the effect of knee direction on bipedal robot running efficiency," *Bioinspiration Biomimetics*, vol. 10, no. 1, 2015, Art. no. 016011.

[27] S. Safdarnejad, J. Hedengren, N. Lewis, and E. Haseltine, "Initialization strategies for optimization of dynamic systems," *J. Comput. Chem. Eng.*, vol. 78, pp. 39–50, 2015.

[28] C. Hubicki, M. Jones, M. Daley, and J. Hurst, "Do limit cycles matter in the long run? Stable orbits and sliding-mass dynamics emerge in task-optimal locomotion," in *Proc. IEEE Int. Conf. Robot. Autom.*, Seattle, WA, USA, 2015, pp. 5113–5120.

[29] GAMS Development Corporation, "Generic Algebraic Modeling System (GAMS)," 24.4.6, Washington, DC, USA, 2015.

[30] A. Wachter and L. Biegler, "On the implementation of a primal-dual interior point filter line search algorithm for large-scale nonlinear programming," *Math. Program.*, vol. 106, no. 1, pp. 25–57, 2006.

[31] C. Fisher, S. Shield, and A. Patel, "The effect of spine morphology on rapid acceleration in quadruped robots," in *Proc. IEEE/RSJ Int. Conf. Intell. Robots Syst.*, 2017, pp. 2121–2127.

[32] C. Santos and V. Matos, "Gait transition and modulation in a quadruped robot: A brainstem-like modulation approach," *Robot. Auton. Syst.*, vol. 59, no. 9, pp. 620–634, 2011.

[33] F. Diedrich and W. Warren, "Why change gaits? Dynamics of the walk-run transition," *J. Exp. Psychol., Human Perception Perform.*, vol. 21, no. 1, pp. 183–202, 1995.

[34] M. Srinivasan, "Fifteen observations on the structure of energy-minimizing gaits in many simple biped models," *J. Roy. Soc. Interface*, vol. 8, no. 54, pp. 74–98, 2011.

[35] M. Srinivasan and A. Ruina, "Computer optimization of a minimal biped model discovers walking and running," *Nature*, vol. 439, pp. 72–75, Jan. 2006.